

Three-dimensional Echo-planar MR Spectroscopic Imaging at Short Echo Times in the Human Brain¹

PURPOSE: To demonstrate the feasibility of three-dimensional echo-planar spectroscopic imaging (EPSI) at short echo time (13 msec) with a conventional clinical imager in the human brain.

MATERIALS AND METHODS: Periodic inversions of a readout gradient were used during data acquisition to simultaneously encode chemical shift and one spatial dimension in one excitation. Aliasing artifacts were avoided with a modified acquisition-and-processing method based on oversampling. A double outer-volume suppression technique that adapts to the ovoid brain shape was used to strongly reduce extracranial lipid resonances.

RESULTS: Three-dimensional spatial encoding in vivo of eight sections with 32×32 voxels each (0.75 cm^3) was performed in 34 minutes with four signal averages. The spectral resolution and signal-to-noise ratio (S/N) of resonances of inositol, choline, creatine, glutamate and glutamine, and N-acetyl aspartate were consistent with those previously recorded with conventional phase encoding.

CONCLUSION: EPSI substantially reduces acquisition time for three-dimensional spatial encoding and yields a spectral quality similar to that obtained with conventional techniques without affecting the S/N per unit time and unit volume.

Index terms: Brain, MR, 13.12145, 15.12145 • Magnetic resonance (MR), pulse sequences • Magnetic resonance (MR), rapid imaging • Magnetic resonance (MR), spectroscopy, 13.12145, 15.12145 • Magnetic resonance (MR), three-dimensional, 13.12145, 15.12145

Radiology 1994; 192:733-738

PROTON spectroscopic imaging (SI) can map metabolite signal intensity distributions in the human brain (1-12). Local changes in metabolite levels have been shown in patients with various abnormalities such as brain tumor (1,6,8,10), multiple sclerosis (5,10), brain infarction (7), epilepsy (2), and acquired immunodeficiency syndrome (4). Most results have been obtained with long echo times (TEs) (272 msec) for reasons of technical feasibility. However, the spectral information content decreases strongly with TE because of T2 and J coupling. SI performed with short TEs is advantageous because it provides additional spectral information that is not available with long TEs (10).

To better accommodate patient cooperation in the clinical setting, recent technical developments have sought to reduce the generally long acquisition times necessary for SI. Three-dimensional phase encoding is desirable because it yields complete volume coverage, permits the acquisition of thin sections (albeit with a sinc profile), and avoids chemical shift artifacts. However, phase encoding is time-consuming. To shorten data acquisition times, multisection techniques have been introduced as an alternative, but the number of sections that may be imaged with these techniques is limited because of the long data-acquisition window (11). More recently, shorter acquisition times have been achieved by the acquisition of multiple individually phase-encoded echoes during a single excitation (12). This method increases the signal-to-noise ratio (S/N) per unit time and unit volume but intro-

duces variable T2 weighting in the k-space and is not compatible with short-TE acquisitions. Alternative methods in which fast imaging performed with a Dixon-type TE shifting (13-15) is used to encode spectral information have been proved to be feasible, although at the expense of spectral resolution. These methods are not suitable for short-TE acquisitions.

Echo-planar spectroscopic imaging (EPSI), an elegant method proposed by Mansfield, is the fastest encoding scheme known (16) and permits complete three-dimensional spatial encoding in a clinically reasonable time. EPSI, however, requires strong, fast switching gradients with excellent eddy current performance. Readout gradients are periodically inverted during the acquisition of the spectroscopic echo to simultaneously encode chemical shift and space in a single excitation. So far, spectral aliasing artifacts and localization constraints due to gradient limitations have precluded applications beyond the initial feasibility studies (17-22).

We have implemented EPSI in the human brain on a conventional clinical

Abbreviations

Cho	choline
Cr	creatine
DQA	daily quality assurance
EPSI	echo-planar spectroscopic imaging
Glx	glutamate/glutamine
GRE	gradient-recalled echo
Ino	inositol
NAA	N-acetyl aspartate
Prot	cytosolic proteins
RF	radio frequency
SI	spectroscopic imaging
S/N	signal-to-noise ratio
SS	spatial suppression
TE	echo time
TM	mixing time
TR	repetition time
WS	water suppression

¹ From the Department of Diagnostic Radiology (S.P., D.L.B.), Warren Grant Magnuson Clinical Center, Bldg 10, Rm 1 C 660, National Institutes of Health, Bethesda, MD 20892; and Laboratory of Neuroscience, National Institute on Aging, National Institutes of Health (C.D.). Received November 22, 1993; revision requested January 24, 1994; revision received April 4; accepted May 2. Address reprint requests to S.P.

© RSNA, 1994

cal imager. The development was guided by the desire to maintain a high spectral resolution, sample an adequate spectral width, avoid aliasing, achieve a spatial resolution consistent with current S/N constraints in acquisition of metabolic images, and obtain the shortest TE possible. Spectral aliasing and localization artifacts, which often occur in conventional EPSI and which are due to gradient constraints and interactions with magnetic field inhomogeneities, are avoided by means of a modified data acquisition and reconstruction method based on spectral-spatial oversampling, which separates echoes from positive and negative readout gradients while it maintains an adequate spectral width. Sensitivity and gradient slew rate effect on spectral and spatial resolution, as well as interaction with static magnetic field distortions, were investigated and characterized. To encompass a larger volume of brain parenchyma without the introduction of lipid artifacts from surrounding regions, we developed a double-volume prelocalization scheme. Effective lipid suppression at short TEs is achieved with double outer volume suppression outside an octagonal volume of interest in combination with a section selection based on a stimulated-echo pulse sequence. We demonstrate that short TE EPSI performed in the human brain with three-dimensional spatial encoding and small voxel sizes (0.75 cm^3) in clinically acceptable acquisition times (eg, 34 min) is feasible with this method.

MATERIALS AND METHODS

Pulse Sequence Design

The EPSI pulse sequence (Fig 1) consists of four parts: (a) a three-pulse sequence to generate a stimulated echo from a section of interest, (b) water suppression that is repeated during mixing time (TM) (water suppression intervals one [WS1] and two [WS2]), (c) spatial suppression that is repeated during TM (spatial suppression intervals one [SS1] and two [SS2]), and (d) a spatial-encoding scheme that uses both echo-planar spatial and spectral encoding and conventional-phase encoding.

The stimulated-echo localization scheme was chosen because it is possible to use additional spectral-spatial suppression during TM and for the feasibility of short TEs. All three stimulated-echo section-selective pulses select the same section. Thus, in contrast to conventional stimulated-echo acquisition mode localization schemes (23–25), the magnetization above and below the volume of interest is not perturbed (not disturbed during the pulse sequence); therefore, gradient dephasing requirements and motion sensi-

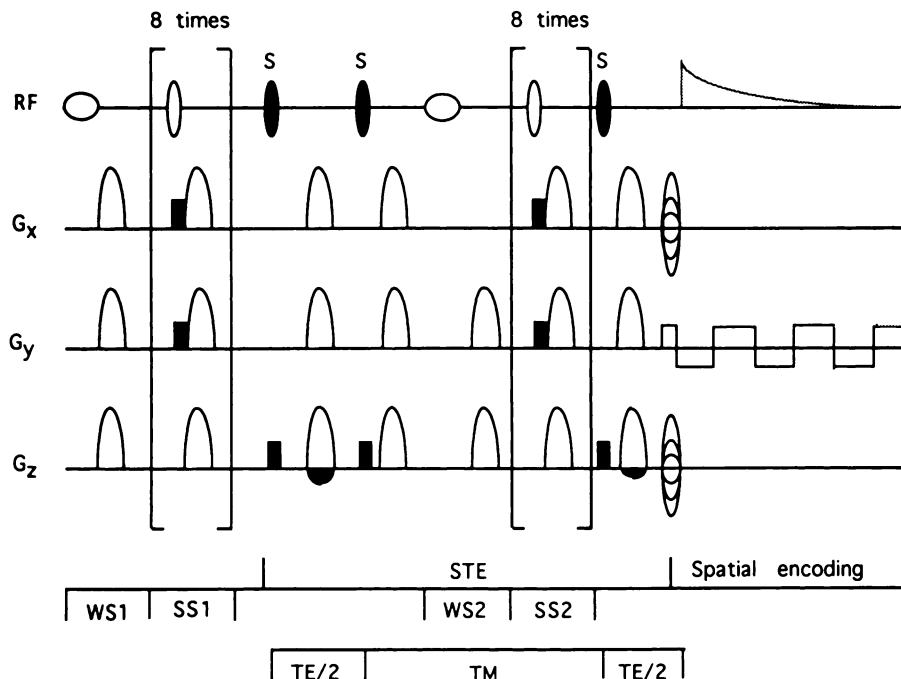


Figure 1. EPSI pulse sequence with flexible double-outer volume suppression. The pulse sequence is based on a stimulated echo localization scheme in which all three radio-frequency (RF) pulses (gray symbols labeled S) select the same section. Spatial suppression (indicated by spatial suppression intervals 1 [SS1] and 2 [SS2]) is applied orthogonal to the stimulated echo-selected section to suppress superficial lipid signals. Multiple ($n = 8$) spatial suppression pulses with subsequent gradient dephasing are applied during each suppression period (SS1 and SS2) in different spatial orientations to follow the contours of the brain. Two chemical shift selective water suppression pulses (WS1 and WS2) are applied. Spatial localization is achieved by means of echo-planar spectral-spatial encoding in one spatial dimension and by phase encoding in the other dimensions. G_x = x gradient, G_y = y gradient, G_z = z gradient.

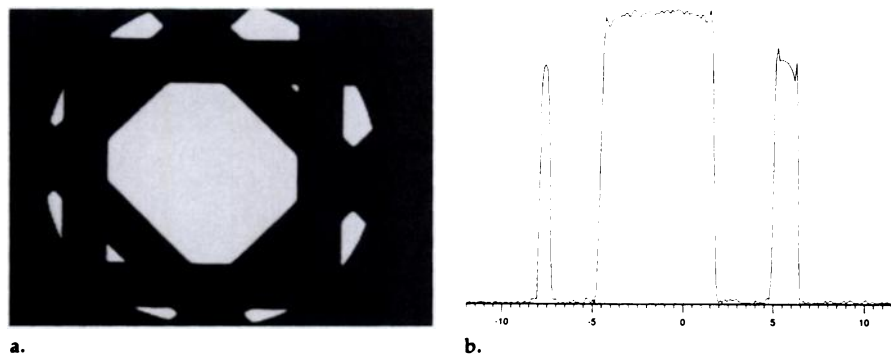
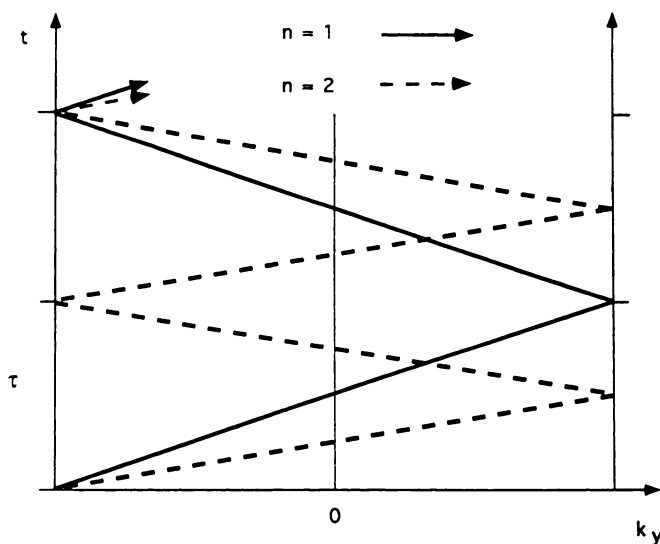


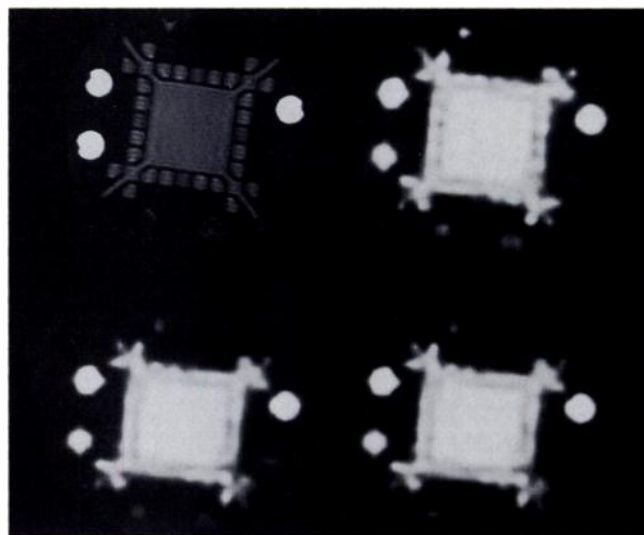
Figure 2. Spatial suppression on a circular phantom. (a) Phantom image obtained with eight suppression sections around a central volume of interest (24-cm field of view). (b) Suppression section profile in a selected line from (a) demonstrates the uniformity of the suppression. Residual signals are at the noise level. The overall phantom profile is slightly rounded because of RF inhomogeneities. Scale indicates centimeters.

tivity are reduced despite the lengthened TM for additional water and spatial suppression. Stimulated-echo radio-frequency (RF) pulses of 2 msec, gradient ramps of $500 \mu\text{sec}$, and gradient crusher pulses of 2 msec were used to produce TEs as short as 10 msec. Chemical shift selective pulses with a bandwidth of 75 Hz were used for water suppression. Sixteen 3-msec spatial-suppression pulses (eight in each suppression interval [SS1 and SS2]) with subsequent 4-msec gradient-dephasing pulses were used to obtain flexible suppression of multiple 4-cm-thick sections around the

volume of interest and orthogonal to the stimulated echo-selected section. The positions of the suppression sections were along the contours of the brain and were chosen to include as much gray matter as possible inside the perselected volume. An example of the spatial suppression on a phantom is shown in Figure 2a. The position, orientation, and width of each suppression section was adjusted individually by means of a graphic interface. The flip angles of the water- and spatial-suppression pulses were adjusted to compensate for T1 effects. On phantoms, uniform, sev-



3.



4.

Figures 3, 4. (3) The k_y - t -space trajectories of EPSI acquisition methods with different spatial-spectral oversampling ratios (n). (The subdomain of the total four-dimensional data space that contains spatial encoding along the k_y axis and spectral encoding along the time axis is defined as k_y - t -space.) The time interval τ determines the desired spectral width $\frac{1}{2}$ in the reconstructed spectra. The other k -space domains, which are orthogonal to the k_y - t plane, are not shown. (4) Comparison between conventional SI and EPSI performed in a daily quality assurance (DQA) phantom. Top left: GRE localizer image (100/5; flip angle, 45°; field of view, 24 cm). Top right: Conventional MR spectroscopic image obtained with two-dimensional phase encoding in 32 minutes (2,000/13; TM, 120 msec; two signals averaged; matrix, 32 × 32). This image was obtained by integration over the entire spectral range. The images in the bottom row (2,000/13; TM, 120 msec; two signals averaged; matrix, 32 × 32) consist of EPSI data acquired in 1 minute: Bottom left: Integrated image reconstructed from even echo data. Bottom right: Integrated image reconstructed from odd echo data.

eral-hundred-fold spatial suppression was achieved. The width of the transition regions from minimum to maximum suppression was less than 10% of the saturation section width (Fig 2b).

For echo-planar spatial-spectral encoding, a trapezoidal readout gradient was inverted periodically to encode the k space in a zigzag trajectory (Fig 3). The solid-line trajectory corresponds to the original encoding scheme proposed by Mansfield (16), in which the length of each trapezoid (τ) corresponds to the inverse of the spectral width in the reconstructed spectra. In time, spectral and spatial information convolves, which leads to chemical shift artifacts. A reversal of the readout gradient in the presence of local magnetic field inhomogeneities and asymmetries in gradient switching introduce periodicities in k space that cause aliasing artifacts. Aliasing can be removed by the separation of the echoes obtained with positive and negative gradients at the expense of a reduction in the spectral width to $\frac{1}{2}\tau$ (16,18,19,21). To simultaneously reduce chemical shift artifacts and eliminate aliasing while retaining the desired spectral width ($\frac{1}{2}$), we use spatial-spectral oversampling, as represented by the dotted-line trajectory in Figure 3, with the separation of even and odd echoes during reconstruction. When an oversampling ratio of 2 is used, the strength of the readout gradient is doubled, which reduces chemical shift artifacts twofold. After the separation of even and odd echoes and the time inversion of echoes obtained with negative gradients, the two data sets are reconstructed separately, and the results are added together to maintain the S/N.

The method was implemented on a conventional clinical 1.5-T, whole-body imager (Signa; GE Medical Systems, Milwaukee, Wis) with actively shielded gradients of 10-mT/m strength. Echo-planar spatial-spectral encoding was performed along the y axis. At 1.5 T, a spectral width ($\frac{1}{2}$) of 488 Hz covers almost all resonances that are observable in vivo (between 0 and 7.64 ppm). With an oversampling ratio of 2, the duration of each readout gradient lobe ($\frac{1}{2}$) was 1,024 μ sec. For spatial resolutions of 5–10 mm, the readout gradient amplitudes were 4.6–2.3 mT/m, and the gradient ramp times from zero to maximum amplitude were limited to between 160 and 80 μ sec (slew rate, approximately 29 T/msec) because of the hardware used. Because of the convolution of spatial and spectral information, the water signal could be positioned on resonance, and any spectral resonance outside a frequency range of ± 244 Hz would alias back into the spectrum. For each data trace, 16,384 complex data points (512 spectral points × 32 spatial points) were sampled continuously with a data bandwidth of 32 kHz to yield a frequency resolution of 1.9 Hz. Data acquisition and echo-planar gradient encoding started 1 msec before the top of the stimulated echo to minimize first-order phase errors in the spectra. No gradient tuning was required. The x and z dimensions were localized with conventional-phase encoding.

Imaging Protocol

Measurements were obtained by means of a standard quadrature birdcage head coil on healthy volunteer subjects. Before

measurement, informed consent was obtained from all subjects in accordance with review protocols at our institution. Food and Drug Administration guidelines for the deposition of RF power were observed, and hearing protection was provided. Rapid multisection gradient-recalled echo (GRE) images were obtained with a repetition time (TR) of 100 msec and a TE of 5 msec (TR/TE = 100/5) for localization of a volume of interest. A 4.5-cm-thick axial slab at the level of the lateral ventricle was preselected. First- and second-order shimming on the volume of interest was performed manually. EPSI data were acquired with the following parameters: 2,000/13; TM, 120 msec. A 32 × 32 × 8 k -space matrix was sampled with a 32 × 32 × 6-cm³ field of view with four signals averaged. The nominal voxel size was 0.75 cm³. The total data acquisition time was 34 minutes.

Data Processing

Data were processed with commercially available software (SA/GE; GE Medical Systems, Milwaukee, Wis) on a commercially available workstation (Sparc II; Sun Microsystems, Mountain View, Calif). Data that represented even and odd echoes were separated into separate data sets and were reconstructed separately. Each edited echo-planar data trace was reformatted into a two-dimensional submatrix to separate spatial and spectral information. Spectral filtering consisted of a 2-Hz exponential line broadening. Spatial filtering consisted of the use of a Fermi function (radius; $0.9k_{max}$ and width, $0.2k_{max}$ where k_{max} = the maximum encoded k -

space value along a given spatial direction) to reduce Gibb ringing. Residual water resonances were removed by low-frequency filtering in the time domain: A binomial filter 131 points wide was applied to the spatially localized time-domain data, and the result was subtracted from the original time-domain data. This strongly reduced residual water resonances and had a negligible effect on metabolite resonances outside a spectral range of 3.9–5.5 ppm. Local shifts in peak position due to inhomogeneities in the magnetic field strength were automatically corrected by means of referencing to the position of *N*-acetyl aspartate (NAA). Zero-order phase correction was performed automatically. Even- and odd-echo absorption mode spectra were added to maintain the S/N. Spectroscopic images were created in the magnitude mode by means of spectral integration over a spectral width of 12 Hz.

RESULTS

To compare the performance of the EPSI encoding scheme with that of conventional phase-encoded SI, we performed non-water-suppressed planar encoding with 32×32 pixels (the phase encoding gradient in the *z* direction was switched off) and resolutions between 10 mm and 5 mm on a DQA phantom (GE Medical Systems) that contained water and glycerol (Fig 4). There was no major difference in the spatial localization achieved by means of EPSI in 1 minute (Fig 4c,d) and that achieved by means of conventional-phase-encoded SI in 32 minutes (Fig 4b). A slight loss in spatial resolution due to continuous data sampling during the gradient ramps (10%–20%, which depends on the gradient ramp time) was only apparent before spatial filtering was performed. The spectral resolution over the entire plane was comparable and spectral artifacts due to residual eddy currents were very similar (Fig 5), which suggests that most eddy current effects were not due to the oscillation of the readout gradient but rather to the strong gradient crusher pulses for volume pre-localization. Aliasing artifacts were absent. The S/N in EPSI performed in 1 minute was approximately four to six times less than that in conventional SI performed in 32 minutes, a result consistent with the shorter acquisition time. Interactions of magnetic field inhomogeneities with EPSI were investigated with use of linear and nonlinear (shim) gradients in different spatial directions. Frequency shifts of several hundred hertz did not affect spatial localization.

Echo-planar spectroscopic images of the human brain together with the

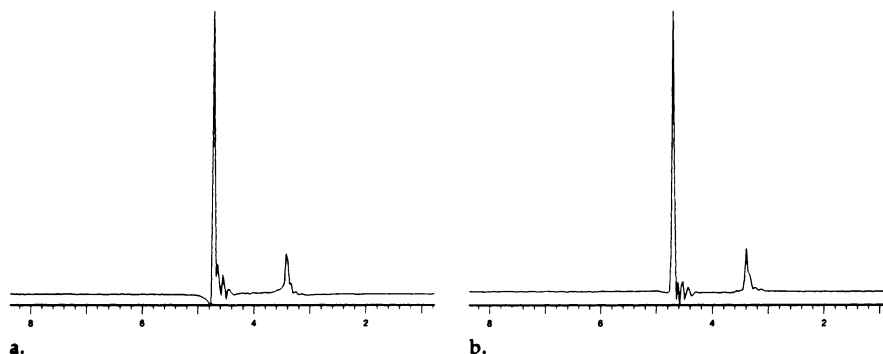


Figure 5. Individual spectra from (a) conventional SI and (b) EPSI of the head phantom. The spectra were obtained from the data sets shown in Figure 4. The two resonances represent water (on resonance) and glycerol (off resonance). The EPSI spectrum was obtained by the addition of absorption mode spectra from even and odd echo data sets. The total spectral range of approximately 7.7 ppm is shown and demonstrates the absence of aliasing artifacts. Little evidence exists for additional eddy current effects because of the echo-planar readout gradients (see distortions to the right of the water line).

corresponding localizer images are shown in Figure 6. Because of the short TE used in this study, it was possible to detect singlet resonances from choline (Cho), creatine (Cr), and NAA, as well as multiplet resonances from inositol (Ino), glutamate or glutamine (Glx), and cytosolic proteins (Prot). The spectroscopic images demonstrate relatively homogeneous metabolite distributions in brain tissue within the S/N constraints of the data. In the bottom of section 5, the ventricular spaces are clearly visible. In section 4, partial volume effects reduce the image contrast in the ventricles. Residual water and lipid resonances from superficial regions were strongly reduced to or below the level of the metabolite resonances, except in the top section. Even in that section, they do not markedly bleed into the volume of interest. These resonances are due to difficulties in positioning the suppression sections when large volumes of interest are selected and to chemical shift artifacts from the spatial suppression. These artifacts can be reduced by the use of thinner suppression sections and more-selective RF pulses. The spectral quality was similar to that obtained with conventional methods (10) and was consistent in different voxels, with the exception of spatial variations in line width due to local magnetic field inhomogeneities (Figs 7, 8). The S/N of NAA was between 10 and 15 in well-resolved voxels, a result consistent with results obtained with conventional phase-encoded, planar SI in the same time frame (10).

DISCUSSION

As shown on phantoms, EPSI provides an S/N per unit time and unit

volume that is similar to that obtained with conventional phase-encoded SI at the same bandwidth per data point. The reader can intuitively understand this fact by considering the following one-dimensional example: When echo-planar readout gradients are applied to encode space, the data bandwidth increases according to the number of pixels (*n*) that are encoded, with a concomitant \sqrt{n} increase of the noise. With *n*-fold averaging to match the acquisition time of a conventional phase-encoding scheme, the S/N with EPSI is the same as it is with conventional-phase-encoded SI.

Spectral-spatial oversampling with the separation of even and odd echoes is crucial to the maintenance of the S/N, because without oversampling it is difficult to correct for aliasing artifacts, which might cause destructive interference. EPSI as presented herein is not directly comparable with "conventional" echo-planar imaging, because there is no phase-encoding gradient applied during data acquisition that might interact with magnetic field inhomogeneities. Image distortions, which only occur in the readout direction, are minor and are further reduced by our spectral-spatial oversampling. However, we noted that it is important to apply second-order shim gradients to limit spectral line broadening and frequency shifts whenever data are acquired from large volumes of interest of the brain. Similarly, the use of appropriate postprocessing methods with automatic correction of frequency shifts due to residual magnetic field inhomogeneities improved the representation of the metabolite signal distributions.

Currently available gradient hardware on commercial whole-body imagers is well suited for applications of

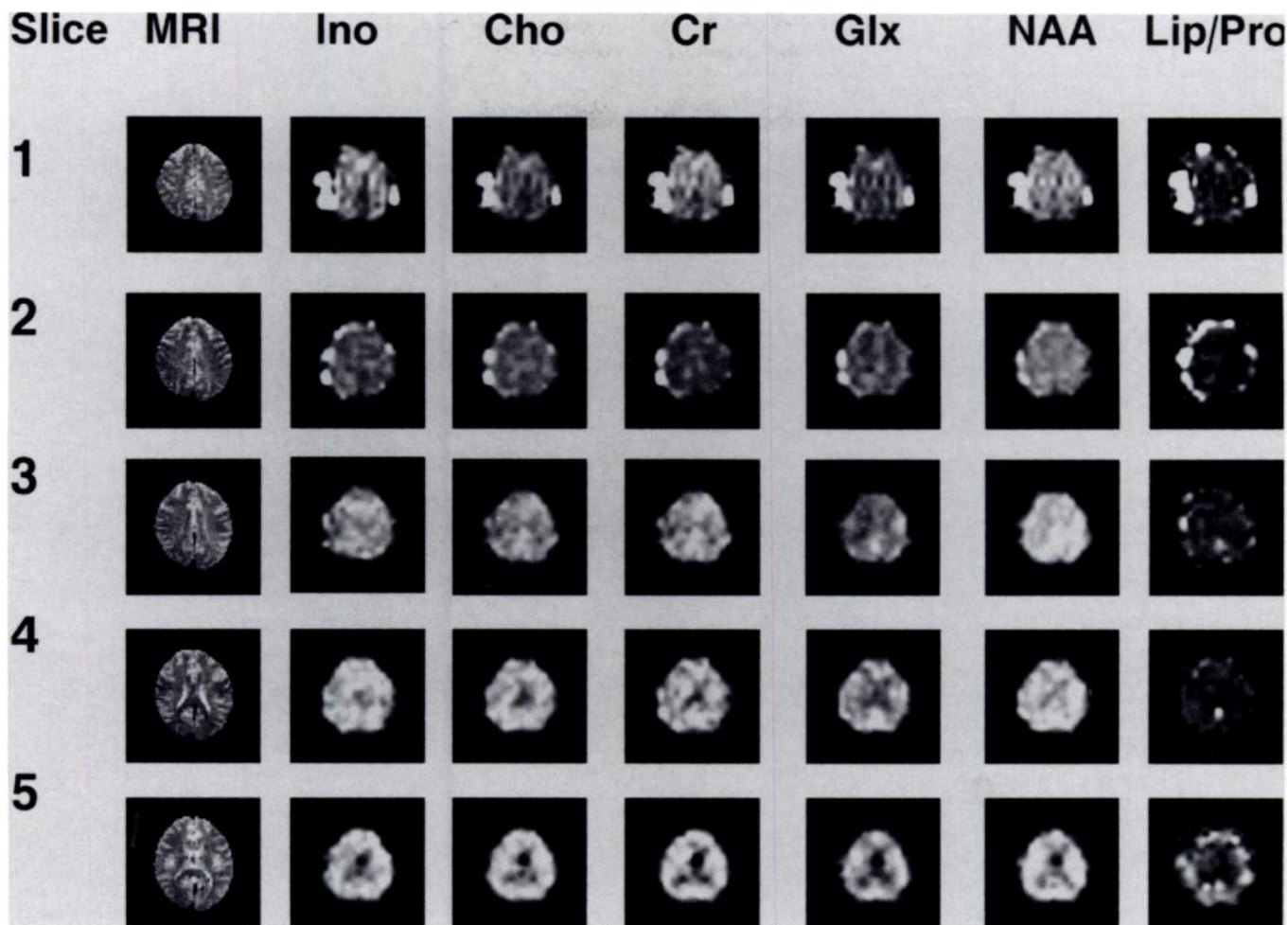


Figure 6. Three-dimensional echo-planar spectroscopic images (2,000/13; TM, 120 msec) obtained in a healthy subject. From a total of eight encoded sections with a nominal section (*Slice*) thickness of 7.5 mm, only the five central sections (1–5) are shown. Spectroscopic images that show the resonance of inositol (*Ino*) (3.56 ppm), choline (*Cho*) (3.24 ppm), creatine (*Cr*) (3.03 ppm), glutamate and glutamine (*Glx*) (2.35 ppm), NAA (2.02 ppm), and cytosolic proteins (*Pro*) (1.3 ppm) and residual lipid (*Lip*) (1.3 ppm) are shown together with the corresponding localizer images (*MRI*). Note the delineation of the ventricles in the bottom section, the flat metabolite distribution in the volume of interest, and the effective lipid suppression despite the short TE.

EPSI in the human brain and does not introduce substantial localization artifacts and spectral distortions. Active gradient shielding, as well as the use of powerful and stable gradient amplifiers, is crucial to achieve the required gradient performance. To achieve a spatial resolution higher than 5 mm, it will be necessary to achieve higher gradient slew rates (eg, with dedicated head gradient sets or more powerful gradient amplifiers). Stronger gradients are available on small-bore imagers, but higher field strengths and smaller voxel dimensions impose additional gradient constraints.

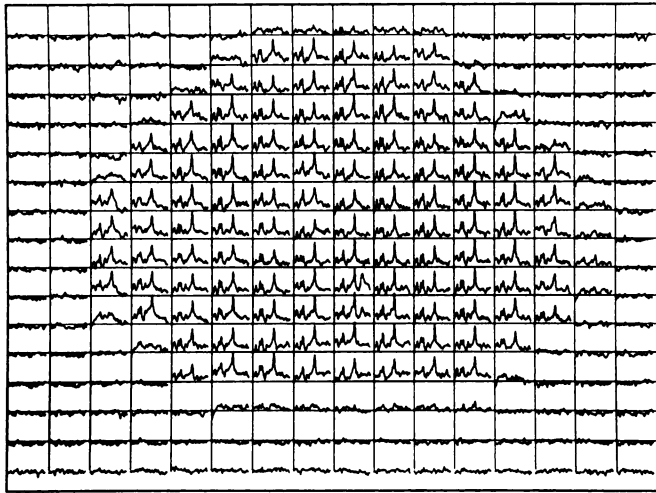
EPSI can help to control motion artifacts by restricting them to the phase-encoding dimensions. With many SI techniques, strong dephasing gradients are used for spatial prelocalization. They introduce additional (intraview) motion sensitivity, which may be a problem in uncooperative

patients. A recently proposed compensation method for intraview motion sensitivity (26) has been shown to be particularly effective for small bulk translations during the spatial prelocalization sequence. Artifacts from nonlinear movements, which are more difficult to compensate for, can be reduced more effectively with EPSI. This technique may enable measurement in moving organs, such as the heart, and diffusion-sensitive SI, which is extremely sensitive to motion (27).

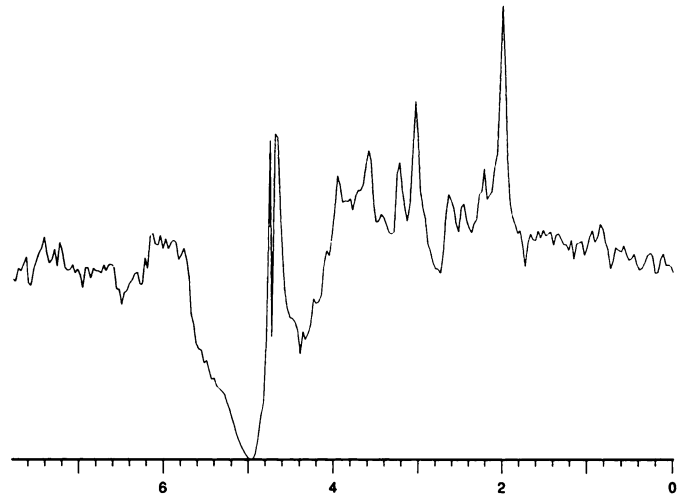
EPSI is particularly useful in cases in which the S/N is already adequate to allow for faster encoding or in which additional spatial dimensions need to be encoded in the same time frame. With the technique presented herein, we could have acquired spectra from the entire brain (32 sections) in the same acquisition time. With conventional methods, this would have taken several hours. The current

limitations of three-dimensional EPSI are the difficulty of shimming over large brain volumes, the increasing complexity of the spatial-suppression scheme with increasing size of the volume of interest, and the difficulty in automatic processing of large data sets. Even in this experiment, the data size was 32 Mbyte. Fully automatic methods of data processing are required for routine applications. The increased acquisition speed may be more fully exploited as phased-array surface coils and higher field strengths become available. This may ultimately lead to functional EPSI with a time resolution of a few minutes.

More general applications of EPSI include fast shimming and quantitative fat and water imaging. Phase-sensitive GRE imaging is often used for these purposes but has a limited spectral resolution and suffers from modulation effects from fat. For in vivo



7.



8.

Figures 7, 8. (7) Zoomed spectral array from section 4 in Figure 6 that displays a spectral range from 1 to 3.7 ppm, with major resonances from Cho, Cr, and NAA. Note the excellent lipid suppression in the periphery. (8) Individual spectrum from the array in 7. The entire spectral range is displayed. Singlet resonances from Cho (3.24 ppm), Cr (3.03 ppm), and NAA (2.02 ppm), as well as multiplet resonances from Ino (3.56 ppm), Glx (2.35 ppm), and Prot (0–2 ppm), are visible. The residual water peak is not centered, because the spectrum has been rotated to obtain a conventional display. Note the absence of aliasing artifacts.

shimming, a spatial resolution of several millimeters is adequate, and EPSI is a fast alternative that permits easy distinction between water and fat. For quantitative fat and water imaging, it may be desirable to resolve the fat spectrum, which consists of several resonances. EPSI is an alternative to the more qualitative Dixon-type GRE techniques. Future implementation of EPSI will benefit from more powerful whole-body gradients that will soon be available for echo-planar imaging. ■

Acknowledgments: We thank Jeffrey R. Alger, PhD, for stimulating discussions and encouragement during this study. Gioacchino Tedeschi, MD, provided support for volunteer studies. We thank Geoffrey Sobering, MD, and GE Medical Systems for software support.

References

- Luyten PR, Marien AJH, Heindel W, et al. Metabolic imaging of patients with intracranial tumors: H-1 MR spectroscopic imaging and PET. *Radiology* 1990; 176:791–799.
- Luyten PR, van Ryen PC, Meinert LC, Marien AJH, den Hollander JA. Identifying epilepsy (abstr). In: Book of abstracts: society of magnetic resonance in medicine 1990. Berkeley, Calif: Society of Magnetic Resonance in Medicine, 1990; 1009.
- Spielman D, Pauly J, Macowski, Enzman D. Spectroscopic imaging with multidimensional pulses for excitation: SIMPLE. *Magn Reson Med* 1991; 19:67–84.
- Meyerhoff DJ, Duyn JH, Bachman L, Fein G, Weiner MW. Alterations of brain proton metabolites in HIV infection: preliminary 1H SI findings (abstr). In: Book of abstracts: Society of Magnetic Resonance in Medicine 1991. Berkeley, Calif: Society of Magnetic Resonance in Medicine, 1991; 404.
- Arnold DL, Matthews PM, Francis GF, O'Connor J, Antel JP. Proton magnetic resonance spectroscopic imaging for metabolic characterization of demyelinating plaque. *Ann Neurol* 1992; 31:235–241.
- Herholtz K, Heindel W, Luyten PR, et al. In-vivo imaging of glucose consumption and lactate concentration in human gliomas. *Ann Neurol* 1992; 31:319–327.
- Duijn JH, Matson GB, Maudsley AA, Hugg JW, Weiner MW. Human brain infarction: proton MR spectroscopy. *Radiology* 1992; 183:711–718.
- Fulham MJ, Bizzi A, Dietz MJ, et al. Mapping of brain tumor metabolites with proton MR spectroscopic imaging: clinical relevance. *Radiology* 1992; 185:675–686.
- Moonen CTW, Sobering G, van Zijl PCM, Gillen J, von Kienlin M, Bizzi A. Proton spectroscopic imaging of human brain. *J Magn Reson* 1992; 98:556–575.
- Posse S, Schuknecht B, Smith ME, van Zijl PCM, Herschkowitz N, Moonen CTW. Short echo time proton MR spectroscopic imaging. *J Comput Assist Tomogr* 1993; 17:1–14.
- Duyn JH, Gillen J, Sobering G, van Zijl PCM, Moonen CTW. Multisection proton MR spectroscopic imaging of the brain. *Radiology* 1993; 188:277–282.
- Duyn JH, Moonen CTW. Fast proton spectroscopic imaging of human brain using multiple echoes. *Magn Reson Med* 1993; 30:409–414.
- Haase A, Matthaei D. Spectroscopic FLASH imaging (SPLASH imaging). *J Magn Reson* 1987; 71:550–553.
- Twieg DB. Multiple-output chemical shift imaging (MOCSI): a practical technique for rapid spectroscopic imaging. *Magn Reson Med* 1989; 12:64–73.
- Norris D, Dreher W. Fast proton spectroscopic imaging using the sliced k-space method. *Magn Reson Med* 1993; 30:641–644.
- Mansfield P. Spatial mapping of chemical shift in NMR. *Magn Reson Med* 1984; 1:370–386.
- Guilfoyle DN, Mansfield P. Chemical shift imaging. *Magn Reson Med* 1985; 2:479–489.
- Matsui S, Sekihara K, Kohno H. High-speed spatially resolved high-resolution NMR spectroscopy. *J Am Chem Soc* 1985; 107:2817–2818.
- Matsui S, Sekihara K, Kohno H. High-speed spatially resolved NMR spectroscopy using phase-modulated spin-echo trains: expansion of the spectral bandwidth by combined use of delayed spin-echo trains. *J Magn Reson* 1985; 64:167–171.
- Doyle M, Mansfield P. Chemical shift imaging: a hybrid approach. *Magn Reson Med* 1987; 5:255–261.
- Matsui S, Sekihara K, Kohno H. Spatially resolved NMR spectroscopy using phase-modulated spin-echo trains. *J Magn Reson* 1986; 67:476–490.
- Webb P, Spielman D, Macowski A. A fast spectroscopic imaging method using a blipped phase encode gradient. *Magn Reson Med* 1989; 12:306–315.
- Granot J. Selected volume excitation using stimulated echoes (VEST): applications to spatially localized spectroscopy and imaging. *J Magn Reson* 1986; 70:488–492.
- Kimmich R, Hoepfel D. Volume selective multipulse spin echo spectroscopy. *J Magn Reson* 1987; 72:379–384.
- Frahm J, Merboldt KD, Haenicke W. Localized proton spectroscopy using stimulated echoes. *J Magn Reson* 1987; 72:502–508.
- Posse S, Cuenod CA, Le Bihan D. Motion artifact compensation in 1H spectroscopic imaging by signal tracking. *J Magn Reson* 1993; 102B:222–227.
- Posse S, Cuenod CA, Le Bihan D. Human brain: proton diffusion MR spectroscopy. *Radiology* 1993; 188:719–725.